# ICESat LASER ALTIMETER POINTING , RANGING AND TIMING CALIBRATION FROM INTEGRATED RESIDUAL ANALYSIS: A SUMMARY OF EARLY MISSION RESULTS

Scott B. Luthcke, David D. Rowlands,
NASA Goddard Space Flight Center

Claudia C. Carabajal
NVI Inc.

David J. Harding
NASA Goddard Space Flight Center

Jack L. Bufton
NASA Goddard Space Flight Center (ret.)

Teresa A. Williams
Raytheon ITSS

## ABSTRACT

On January 12, 2003 the Ice, Cloud and land Elevation Satellite (ICESat) was successfully launched into orbit. The ICESat mission carries the Geoscience Laser Altimeter System (GLAS), which consists of three near-infrared laser transmitters to be operated sequentially over the lifetime of the mission at 40 short pulses per second. The instrument has collected precise elevation measurements of the ice sheets, the ocean surface and land topography as well as observations of sea ice roughness and thickness and surface reflectivity. The accurate geolocation of GLAS's surface returns, the spots from which the laser energy reflects on the Earth's surface, is a critical issue in the scientific application of these data. Pointing, ranging, timing and orbit errors must be compensated to accurately geolocate the laser altimeter surface returns. Towards this end, the laser range observations can be fully exploited through a combined reduction of the various data types to accurately calibrate these instrument parameters required for geolocation. Early mission ICESat data have been simultaneously processed as direct altimetry from ocean sweeps along with dynamic crossovers resulting in a preliminary calibration of laser pointing, ranging and timing. The calibration methodology and early mission analysis results are summarized in this paper along with planned calibration activities.

## INTRODUCTION

To further extend the capabilities of NASA's Earth Observing System (EOS) of satellites, the Ice, Cloud and Land Elevation Satellite was successfully launched into orbit on January 12, 2003. ICEsat orbits the Earth in a ~600 km altitude near-circular orbit with a 94° inclination. The satellite carries the Geoscience Laser Altimeter System (GLAS). This instrument consists of three two-channel lasers to be operated sequentially over the life of the mission. Altimeter-derived surface and cloud elevations are obtained from the 1064 nm near-infrared channel, while cloud and aerosol atmospheric profiles are derived from the 532 nm channel. The surface spot size is approximately 60 m in diameter with an along-track spacing of 172 m. The near-infrared channel makes it possible to obtain precise elevation measurements of the ice sheets, the ocean surface and land topography as well as observations of sea ice roughness and thickness and surface reflectivity.

The laser-altimeter system measures the time of flight of the laser pulse and records the backscatter waveform, digital time series of the returned laser pulse energy. The time of flight determines the range to the surface return, which coupled with the knowledge of the position and pointing of the laser enables the position of the surface return and elevation of the surface at that location to be computed. Analysis of the waveform, a measure of the within-footprint height distribution of illuminated surfaces, is used to further refine the estimate of range, and therefore surface elevation, and to characterize surface relief due to slope and/or roughness and vegetation cover.[1]

In order to observe ice sheet elevation change over time, ICESat requires decimeter single footprint elevation

accuracy on low sloping ice sheet topography. This is the primary driver for high-accuracy (< 5 m horizontal) geolocation of the laser surface return, the spot from which the laser energy reflects on the Earth's surface. A secondary driver for high-accuracy geolocation is the small laser footprints and the small spatial scale over which the surface characteristics of interest vary. The 60 m ground spot size of the laser altimeter is over 30 times smaller than spaceborne radar altimeters currently in use (e.g. Jason-1, TOPEX/Poseidon). It is important to associate the surface characteristics within each small footprint derived from the waveform with a specific location on the Earth's surface. Therefore, accurate geolocation of the surface return is a critical issue in the scientific application of spaceborne laser altimeter data. The geolocation of the laser surface return is computed from the laser-altimeter surface range observation along with the precise knowledge of the spacecraft position, instrument tracking points, spacecraft attitude, laser pointing and observation times. This would be a straightforward computation except for the fact that these data have errors and their pre-launch parameter values and models must either be verified or more likely corrections must be estimated once the instrument is in orbit.[2] ICESat is no exception and pointing, ranging and timing corrections must be calibrated and validated post-launch.

In order to support the calibration and validation of these geolocation parameters several techniques have been developed including: (1) detailed measurements over small target areas, (2) aircraft under-flights and (3) integrated residual analysis.[1] The integrated residual analysis approach is described and applied in this paper. In this approach, orbit and instrument parameters (pointing, ranging and timing) are simultaneously estimated from a combined reduction of laser range and spacecraft tracking data. The laser range data are processed in the form of direct altimetry and dynamic crossover observations. The integrated residual analysis approach has been successfully applied to Shuttle Laser Altimeter (SLA) and Mars Global Surveyor (MGS) laser altimeter data significantly improving the resulting geolocation accuracy.[2,3] Details of the integrated residual analysis methodology and measurement models can be found in Luthcke et al.(2002), Luthcke et al.(2000) and Rowlands et al.(2000).[2, 4, 5] However, for completeness, the methodology will be briefly summarized in this paper before the preliminary ICESat instrument parameter calibration analysis is discussed.

**SYMBOLS**

| | |
|---|---|
| $\boldsymbol{L}_{GCS}$ | Laser pointing unit vector in GLAS Corrdinate System (GCS) |
| $\boldsymbol{L}_{J2000}$ | Laser pointing unit vector in J2000 (celestial reference frame) |
| $\boldsymbol{Lcor}_{J2000}$ | Corrected laser pointing unit vector in J2000 |
| $R_{J2000 \rightarrow GCS}$ | Rotation, J2000 to GCS |
| $R_{GCScor \rightarrow GCS}$ | Rotation, "correction matrix" GCS corrected to GCS |
| $\theta$ | Euler angle (°) |
| $C$ | Euler angle bias parameter (°) |
| $D$ | Euler angle rate parameter (°/s) |
| $Q$ | Euler angle quadratic parameter (°/s^2) |
| $A$ | Amplitude of Euler angle sine term (°) |
| $B$ | Amplitude of Euler angle cosine term (°) |
| $\omega$ | angular frequency, ($2\pi$/T), where T is period of satellite orbit |
| $\Delta t$ | elapsed time within current time period (s) |
| $i$ | Euler angle index (1 = roll, 2 = pitch, 3 = yaw) |
| $j$ | time period index |

**INTEGRATED RESIDUAL ANALYSIS – CALIBRATION METHODOLOGY SUMMARY**

At the core of the integrated residual analysis is NASA/Goddard Space Flight Center's GEODYN precise orbit determination and geodetic parameter estimation system.[6] The laser altimeter range measurement model algorithms have been implemented within the GEODYN system. Therefore, the laser altimeter range processing can take advantage of GEODYN's reference frame modeling, geophysical modeling and its formal estimation process. A

Bayesian least-squares differential correction algorithm is used to iteratively solve for model parameters. Three laser altimeter measurement models have been implemented within the GEODYN system. The first is the classic geolocation measurement model that takes into account the motion of the laser tracking points over the round trip light time of the laser pulse. This measurement model is not directly used for parameter estimation, but is used in constructing the dynamic crossover measurement model and for geolocation file output.

The second measurement model is the dynamic crossover capability. The dynamic crossover measurement model is discussed in detail in Rowlands et al. (1999).[3] To summarize, the dynamic crossover measurement model has been implemented to take into account the small footprint of the laser altimeter along with the observed sloping terrain, and therefore, the horizontal sensitivity of these data. The formulation can exploit change in horizontal crossover location as well as change in radial position of the satellite. It is termed "dynamic crossovers" because, unlike standard radar altimeter crossovers, the pair of observations that form the crossover will likely change as the parameter (e.g. pointing and timing biases) solutions change from iteration to iteration.

Direct altimetry is the third measurement model implemented. The round trip range is computed using knowledge of the spacecraft position, laser pointing, timing and ranging parameters along with a model of surface height. The surface height model is represented by a grid and GEODYN has the capability to ingest multiple surface height grids that can represent various land areas and the ocean surface. The differences between the observed and computed ranges (residuals) are then minimized through the estimation of orbit, pointing, timing and ranging parameters. A detailed discussion and mathematical description of the direct altimetry measurement model can be found in Luthcke et al. (2000).[4]

An important specific application of the direct altimetry measurement model is the ocean sweep calibration maneuver. These calibration maneuvers use specific commanded spacecraft attitude maneuvers and ocean direct altimetry acquired during the maneuver to recover pointing, ranging and timing parameters. The maneuver itself is a small, deliberate roll and pitch deviation of the spacecraft attitude from nominal nadir pointing. The maneuver exploits the relationship between pointing bias and range offset where for a given pointing bias the laser altimeter range offset increases as surface incidence angle increases (Eq. 1, Luthcke et. al. 2000).[4] The contribution from a range bias remains constant and can therefore be separated from the pointing biases. This also protects the pointing bias recovery from surface height modeling errors. The maneuver separates roll and pitch biases by varying roll and pitch out of phase. Varying rates of change in roll and pitch (acceleration and deceleration) also give the maneuver the capability to observe attitude or observation timing biases. The maneuver is performed over the oceans, the elevation of which is well modeled and relatively flat, so that the maneuver enhanced pointing bias contributions to the range residuals can be easily observed. The design of the maneuver and a detailed pre-launch consider covariance error analysis is presented in Luthcke et al. (2000).[4] The analysis shows the maneuver is a strong filter that significantly reduces the impact on pointing bias recovery from errors, such as un-modeled ocean wave structure, that are not close to the maneuver frequency and phase. The error analysis shows pointing corrections can be estimated to the sub-arcsec level for a single maneuver under the worst expected conditions

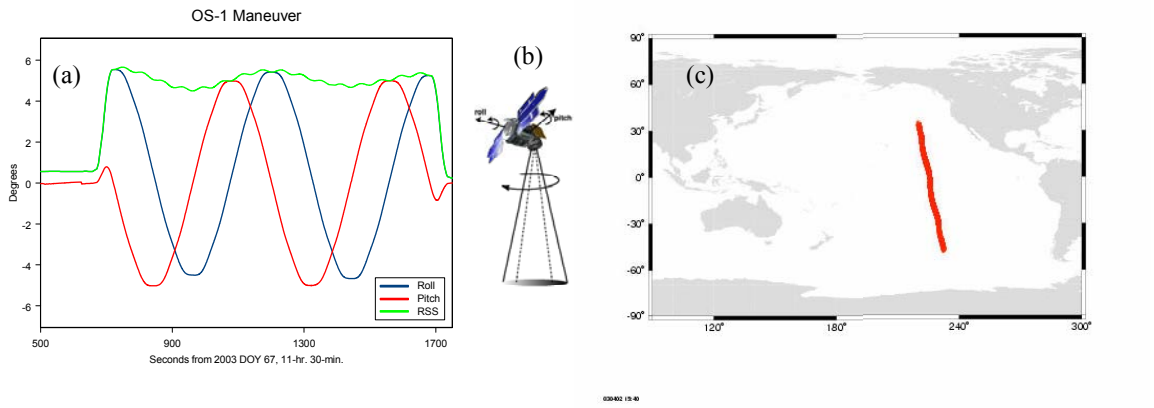


**Figure 1.** (a) ICESat Ocean Sweep maneuver #1 (OS-1) roll and pitch from nominal attitude profile. (b) cartoon of ocean sweep maneuver. (c) geographic location and extent of OS-1.

taking into account a detailed error model. The maneuver can be performed several times sequentially to observe orbital variations in pointing error and can be performed, for example, every day over the course of a mission to observe long-wavelength thermal variations in pointing due to the changing Sun and satellite orbit geometry. The nominal ICESat ocean sweep maneuver consists of two complete ~ 480 s cycles in roll and pitch where roll and pitch are offset in phase by one-quarter of a cycle. Due to operational limitations an octagon, rather than a sinusoid, is used for both roll and pitch to approximate a cone "sweeped" out in space. For ICESat, the amplitude of the "cone" is 3-5 degrees, which corresponds to the optimal range determined by the analysis discussed in Luthcke et al. (2000).[4] The total time for a single maneuver takes approximately twenty minutes. An ICESat ocean sweep maneuver is shown in Figure 1.

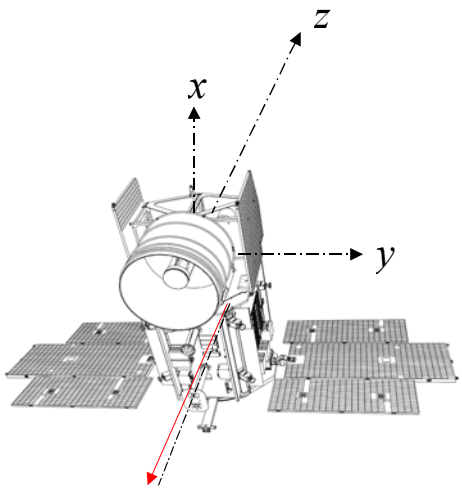


**Figure 2.** GLAS Coordinate System (GCS) summary. Direction of laser pointing shown in red.

It is important to define a common reference and mathematical formulation to support the estimation of pointing corrections. The reference frame must support global and temporal solution comparisons among various groups and techniques. Towards this end we have adopted the GLAS Coordinate System (GCS), which is fixed with respect to the GLAS instrument and also defines the coordinate frame of the instrument optical bench (Figure 2). The a priori or "mission" laser pointing unit vector with respect to the celestial reference frame (CRF), defined as J2000, is computed by the ICESat precision attitude determination (PAD) process which incorporates data from the instrument star tracker (IST) and the stellar reference system (SRS).[7 8 9] The *a priori* or mission pointing vector along with the altimeter derived range and range corrections are provided in the ICESat level 1b and 2 products (e.g. GLA06 data product). In addition, the PAD process also provides a quaternion time series that describes the rotation from the GCS to the CRF at a 10 Hz rate, which we interpolate to the time of each laser shot. Given the adopted reference system and the input data defined above, we can now define a mathematical formulation that describes a set of parameters that allow the computation of a corrected pointing vector from the *a priori* or mission pointing. The corrected pointing for a single laser shot at time $t$ can be expressed as follows.

$$\boldsymbol{L}_{GCS} = R_{J2000 \rightarrow GCS}\, \boldsymbol{L}_{J2000} \qquad (1)$$

$$\boldsymbol{Lcor}_{J2000} = R_{GCS \rightarrow J2000}\, R_{GCScor \rightarrow GCS}\, \boldsymbol{L}_{GCS} \qquad (2)$$

Therefore, in order to compute the corrected laser pointing unit vector ($\boldsymbol{Lcor}_{J2000}$) we must estimate the parameters that comprise the "correction" rotation matrix ($R_{GCScor \rightarrow GCS}$). The correction matrix is implemented within our GEODYN measurement models as a three axis Euler rotation in roll (rotation about GCS ***x***), pitch (rotation about GCS ***y***) and yaw (rotation about GCS ***z*** and rarely used). An Euler angle representation was chosen because it is much more intuitive than a quaternion representation and, because the user has the flexibility to select the order of

rotation, any singularities can be avoided. Equation 3 describes the current parameterization for each of the Euler angles. These parameters can be recovered on a time period basis where different parameter sets can be estimated for each distinct user defined time period. This parameterization can be easily modified to address specific mission scenarios. A more complete description of the GEODYN parameterization is provided in Luthcke et al. (2000 and 2002).[4,2]

$$\theta_{ij} = C_{ij} + D_{ij}\Delta t_j + Q_{ij}(\Delta t_j)^2 + A_{ij}\sin\omega\Delta t_j + B_{ij}\sin\omega\Delta t_j \qquad (3)$$

In practice, there are two references from which we compute the corrected laser pointing unit vector: (1) from the mission pointing as shown in the equations above ($\boldsymbol{L}_{GCS}$,) and (2) with respect to the $z$ axis of the GCS (substitute a 0,0,1 column vector for $\boldsymbol{L}_{GCS}$ in Eq. 2). By design the GLAS laser pointing unit vector will be updated with new estimates of biases and corrections as the mission and calibration analysis progresses. For example, various releases of the GLA06 data product have different laser pointing biases applied as the knowledge of these biases has improved from our calibration analysis. Therefore, the recovered Euler angle correction matrix parameters will be different between these product releases. However, the GCS $z$ axis provides a constant reference to compute the correction matrix. Therefore, we can compute our Euler angle correction parameters with respect to the mission pointing to understand the errors present in the current estimate of the laser pointing, and with respect to the GCS $z$ axis to compare pointing in a common reference frame over the course of the mission.

## EARLY MISSION POINTING, RANGING AND TIMING CALIBRATION

At the time of analysis described here, approximately 36 days of data had been collected from the operation of laser number one in the 8-day repeat calibration orbit. Beginning on February 20, 2003 laser #1 collected approximately 29 days of data while in sailboat attitude mode (GCS $\boldsymbol{y}$ axis along the velocity vector), and another 7 days of data while in airplane attitude mode (GCS $\boldsymbol{x}$ axis along the velocity vector). The spacecraft is periodically reoriented by 90 degrees in yaw to maximize illumination on the solar arrays. During this time period, data from six Pacific ocean sweeps were acquired with two ocean sweeps on each day of year (DOY) 67, 75 and 87. The details of each of the ocean sweeps that acquired data during this initial phase of the mission are given in Table 1. Our initial calibration efforts have focused on the analysis of the ocean sweep direct altimetry range data and dynamic crossovers from a nine-day time period encompassing the four sailboat mode ocean sweeps, comprised of ascending track (nighttime) and descending track (daytime) pairs on DOY 67 and 75. The 9-day time period begins with track 59 of the third ICESat 8-day repeat cycle and ends with track 74 of the fourth 8-day cycle (approximately March 8$^{th}$-17$^{th}$ of 2003) we term this time period "cycle 3.5". While future plans include the processing of crossovers from all available repeat cycles and direct altimetry to precisely mapped surfaces along with the ocean sweeps, the ocean sweeps and cycle 3.5 crossovers are the data selected for our initial calibration analysis presented here.

Table 1. Pacific ocean sweep details.

| Ocean Sweep | DOY 2003 | Night/Day | Maneuver Amplitude | Attitude Mode |
|---|---|---|---|---|
| OS-1 | 67 | Night | 5° | Sailboat |
| OS-2 | 67 | Day | 5° | Sailboat |
| OS-3 | 75 | Night | 3° | Sailboat |
| OS-4 | 75 | Day | 3° | Sailboat |
| OS-5 | 87 | Night | 5° | Airplane |
| OS-6 | 87 | Night | 5° | Airplane |

Our preliminary calibration efforts were focused on removing large-scale pointing biases to provide an initial first-order improvement in geolocation. Towards this end, we analyzed the direct altimeter range data from ocean sweep 1 (OS-1) as soon as these data were made available. The recovered pointing biases are presented in Table 2 along with the solution formal errors. The results are shown relative to both the GCS $z$ axis and the mission pointing provided on release 9 of the GLA06 data product. Figure 3 shows the pre- and post-calibration solution ocean

sweep direct altimetry range residuals computed using a mean sea surface grid derived from over a decade of satellite radar altimetry.[2] The pointing error is quite evident in the pre-calibration residuals (red data points) and a range residual reduction from 10.15 m RMS pre-calibration (red data) to 1.43 m RMS post-calibration (blue data) has been observed.

The pointing bias calibration has been independently validated using a profile matching technique (part of our integrated residual analysis) where digital elevation models (DEMs) of sufficient accuracy and varying topography are compared with ICESat altimeter derived elevation profiles.[10] The profiles are shifted in both the North-South and East-West directions until an optimal match is obtained by minimizing ICESat to DEM elevation residuals. The magnitude of the shift represents a sample estimate of the geolocation accuracy in the horizontal direction. The accuracy of this validation technique is of course limited by the resolution and accuracy of the DEMs used and the limited number of ICESat data points per segment that are compared. Nevertheless, this is a powerful technique for independently validating ICESat geolocation accuracy and therefore instrument/geolocation parameter calibration. Geolocation solutions were validated for various track segments across the US, comparing approx. 1200 points per segment. For example, analysis of a segment of track 87 using 30 m National Elevation Dataset (NED) DEM data and 1177 ICESat elevation observations showed pre-calibration geolocation horizontal accuracy at the level of 160 m. Post-calibration geolocation accuracy (after calibrated pointing biases are applied) was found to be significantly improved and within 1 DEM pixel (< 42 m horizontal RSS) validating our initial integrated residual analysis pointing calibration.[10]

Table 2. OS-1 preliminary pointing calibration.

| Solution Reference | Roll Bias (about GCS x) (arc-sec) | Pitch Bias (about GCS y) (arc-sec) |
|---|---|---|
| GCS $z$ | -199.37 ± 0.05 | 267.69 ± 0.05 |
| Mission pointing | 59.93 ± 0.05 | 14.65 ± 0.05 |

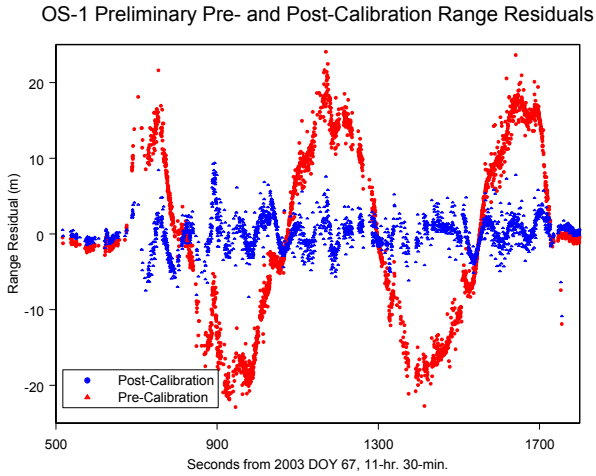


**Figure 3.** OS-1 Pre- (red) and Post- (blue) calibration direct altimetry range residuals. In addition to the large pointing bias signal removed from the pre-calibration residuals, high frequency PAD errors are clearly observed in the post-calibration residuals. A large portion of these PAD errors have now been corrected.

Further analysis of OS-1 along with OS-2, 3 and 4 revealed a complex structure in the post-calibration direct altimetry range residuals with an approximate 60 s period (see Figure 3). The error was observed to be significantly worse during daylight as compared to night. This structure was correlated with the attitude maneuver itself and it was hypothesized that the PAD GCS-to-J2000 quaternions contained the error resulting in a complex high frequency pointing error. Even though the biases had been removed in the initial calibration process, these complex pointing errors remained and could be clearly observed in the ocean sweep analysis (Figure 3). The ICESat PAD products are computed at the Center for Space Research (CSR) at the University of Texas.[8] Researchers at the CSR then used the ocean sweep analysis results as an independent validation of the PAD for correcting and tuning. We performed new ocean sweep analyses for each new PAD solution generated by the CSR team, iterating until a significantly improved PAD solution was found reducing the ocean sweep post-calibration direct altimeter range residuals to the 90 cm RMS level. This particular problem and its eventual solution clearly highlights the power and unique

capability of the ocean sweep maneuver to observe complex errors other than simple biases. In particular the ocean sweep analysis was able to observe high frequency pointing errors that would have been very difficult or impossible to observe using other techniques such as aircraft under-flights and detailed observations in small target areas, profile matching and crossover analysis.

Using the new corrected PAD product and release 11 of the GLAS GLA06 data, which has the pointing biases obtained from the OS-1 analysis (Table 2) applied, we then performed a pointing bias calibration analysis on the four ocean sweep data sets obtained during the sailboat attitude mode. The results of this analysis are shown in Table 3. The results clearly show the OS-1 pointing biases have been properly applied to the GLA06 data product (compare Tables 2 and 3). However, of particular note is the large pointing bias variation observed between data obtained in sunlight versus that obtained in shadow. From this analysis there appears to be a thermally driven pointing variation with a one cycle per revolution (1CPR) mode. This is very similar, but of a much smaller magnitude, to that observed from Shuttle Laser Altimeter (SLA) data analysis.[2] Even so good consistency between solutions separated by 8 days is observed. The remaining residual difference between like solutions separated by 8 days is in part due to slightly different sampling of the day-night variation. Combined solutions for night (from OS-1 and 3) and daylight (from OS-2 and 4) are also presented.

Table 3. Sailboat attitude mode OS pointing calibration summary (release 11 PAD and GLA06 – initial pointing bias shown in Table 2 is applied).

| Solution | Roll Bias (about GCS x) (arc-sec) | Pitch Bias (about GCS y) (arc-sec) | # of observations in solution |
|---|---|---|---|
| OS-1 / Night / DOY 67 | 0.04 ± 0.04 | 0.05 ± 0.04 | 24227 |
| OS-3 / Night / DOY 75 | 2.27 ± 0.04 | 2.02 ± 0.04 | 29271 |
| OS-2 / Day / DOY 67 | -13.70 ± 0.05 | -5.80 ± 0.05 | 20758 |
| OS-4 / Day / DOY 75 | -12.57 ± 0.04 | -9.05 ± 0.05 | 27092 |
| OS-1+3 / Night / 67+75 | 1.10 ± 0.03 | 0.98 ± 0.03 | 53237 |
| OS-2+4 / Day / 67+75 | -13.12 ± 0.03 | -6.92 ± 0.03 | 47439 |

The analysis presented above gave clear evidence that the GLAS altimeter data products still contained a significant variation in pointing error throughout the orbit revolution. Fortunately, because the ocean sweeps occurred in mid-latitudes and the date these data were collected (mid-March), the "noon" and "midnight" of the orbit occurred during the ocean sweeps and provided a sampling of the maximum excursions of the pointing variation. However, this certainly is a limited sampling of the full signal throughout the orbit and we needed to fully account for the time varying pointing error. One way we could capture this ~1CPR signal is to continuously perform ocean sweeps throughout a few orbit revolutions. This situation is very similar to that used for SLA pointing calibration.[2] The resulting direct altimeter range data could then be reduced and pointing biases could be estimated throughout the orbit at small discrete time intervals (~4 minutes) and to sub-arc-sec accuracy. While there are currently plans to execute this full orbit revolution continuous ocean sweep, to date it has not yet been implemented. Therefore, in order to capture the orbital pointing error variation, we simultaneously processed the GLAS direct altimeter range data from the four sailboat mode ocean sweeps along with dynamic crossovers computed using 9-days of data acquired during cycle 3.5. The crossovers are predominantly in the high-latitudes (~90% above 60° latitude), while the ocean sweeps provide a wealth of data in the mid-latitudes. Therefore, processed together, these two data types compliment each other well and provide the ability to observe the pointing variation throughout the orbit revolution

The orbital pointing variation was estimated from a combined reduction of the ocean sweep and crossover data. The resulting pointing solution is an average orbital pointing variation solution over 134 orbits during the March 8$^{th}$ – 17$^{th}$ 2003 time frame. For our initial analysis we represented the orbital pointing variation as a bias and sinusoid estimating $C$, $A$ and $B$ terms for both roll and pitch as shown in Eq. 3. The results are presented in Figure 4 where the pointing angle is shown as a function of orbit angle. Orbit angle is the angle between the satellite position vector

and the sun vector projected in the orbit plane where 0° is orbit 6AM, 90° is orbit noon (directly in line with Sun vector in orbit plane) and 270° orbit angle is orbit midnight (opposite Sun vector in orbit plane). A well determined solution is obtained using the sinusoidal functional form because a total of only 6 parameters are necessary (*C*, *A* and *B* terms for both roll and pitch as shown in Eq. 3). However, further analysis suggests the actual pointing variation is not perfectly sinusoidal in nature. Therefore, we are now in the process of estimating a step function representation of the orbital pointing variation based on a reduction of the ocean sweep and crossover data. The step function will give us the ability to observe the actual shape of the pointing variation. Additionally, continuous ocean sweep maneuvers throughout 1-2 revolutions will provide the necessary data to significantly strengthen a step function solution and to increase its resolution in orbit angle. Still, our preliminary sinusoidal solution presented here captures a significant part of the orbital pointing error variation and represents a major improvement over the current mission pointing and a simple pointing bias solution.

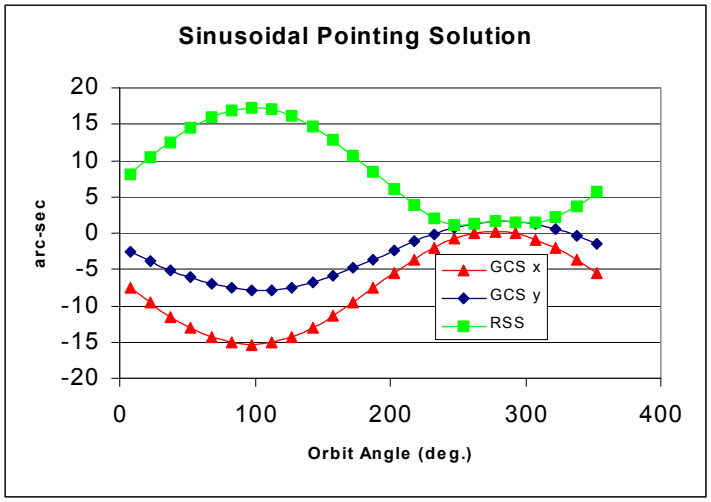


**Figure 4.** Estimated orbital pointing variation (using sinusoidal functional form) from a combined reduction of ocean sweep direct altimetry and dynamic crossover data from March 8th-17th 2003.

Although our efforts have concentrated on pointing calibration during this initial mission calibration effort, we have performed some limited analysis towards calibrating both range and timing. In order to calibrate range bias we performed a reduction of 1 s rate ocean direct altimeter range data from ~9-days during the cycle 3.5 time period. A summary of the range bias recovery is presented in Table 4 and indicates the reported altimeter ranges are too long by 43.2 cm. Of course, this is a function of the altimeter tracking point offset used and the way in which the ranges are computed (waveform centroid) for this particular analysis. By design, pointing bias recovery from ocean sweep direct altimetry is insensitive to timing bias. However, pointing bias recovery from crossovers is sensitive to observation timing bias, and therefore, an observation timing bias must be simultaneously estimated when performing a calibration based on crossover data. Table 4 presents the recovered observation timing bias solution determined from the combined reduction of cycle 3.5 crossover and ocean sweep direct altimeter range data.

Table 4. Preliminary Range and Observation Timing Bias Solution

| Bias Type | Data used | Estimate |
|---|---|---|
| Range | 165357, 1/s ocean direct altimeter range observations | 43.2 ± 0.1 cm |
| Observation Timing Bias | 103126 ocean sweep direct altimeter range and 7441 dynamic crossover observations | 6.5 ± 0.3 ms |

## CONCLUSIONS and FUTURE WORK

From the analysis presented in this paper it is evident that much progress has been made in calibrating the ICESat instrument/geolocation parameters of pointing, ranging and timing. While this analysis is preliminary and based on a limited amount of early mission data we have already significantly improved upon the initial calibration efforts. The ocean sweep technique is shown to be a powerful tool for the calibration of pointing biases at the sub-arc-sec level. In addition, the ocean sweep technique uniquely observed significant high-frequency errors in the early mission PAD solutions that have now been corrected. Analysis of direct altimetry from ocean sweep data taken in both sunlight and shadow has revealed a large (amplitude ~17 arc-sec) thermally driven orbital variation in the pointing. Through the combined reduction of both ocean sweep direct altimeter range and dynamic crossover data we have been able to compute a preliminary calibration of the orbital pointing variation using a sinusoidal representation. Even at this early stage of the mission and calibration efforts, the analysis shows we are very close to the mission pointing requirement of 1.5 arc-sec. A preliminary solution for ranging and timing biases was performed using both direct altimeter range and dynamic crossover data. Range bias was found to be 43.2 cm while the observation timing bias was found to be 6.5 ms.

While significant improvement in pointing, ranging and timing has been realized through this preliminary calibration effort, errors still remain and further improvement will be made. Future efforts will include the estimation of a step function representation of the orbital pointing variation, incorporating SRS data. In addition, a complete analysis of airplane mode pointing, ranging and timing will be performed. An ocean sweep campaign is also planned. During this campaign at least two ocean sweep maneuvers will be performed on each day for an entire 8-day repeat. In addition, the ocean sweep maneuver will be continuously performed for at least one orbit revolution in the 8-day campaign period. These data along with dynamic crossover and SRS data will significantly improve our knowledge of the orbital pointing variation and biases. Additional improvements will be gained from a more detailed waveform analysis and resultant refined range observation to be used in our calibration analysis. A more complete independent validation of our calibration and resultant improved geolocation will be performed using profile and waveform matching techniques. Even with these planned improvements, the preliminary analysis presented in this paper has demonstrated the power of ocean sweeps and dynamic crossovers to calibrate pointing, ranging and timing in the presence of significant errors such as high-frequency PAD errors and large thermally driven orbital variations in pointing. The results emphasize the importance and demonstrate the capability of the integrated residual analysis calibration methodology to fully accommodate not only simple biases but also complex time-varying errors.

## ACKNOWLEDGMENTS

The authors wish to thank the ICESat project for supporting this research effort. The authors also wish to thank the following individuals for the many fruitful technical discussions and various support: B. Schutz, C. Webb, L. Magruder, S. Sirota, J. Abshire, S. Bae and P. Millar. The authors also wish to thank members of the ICESat Science Computing Facility team for their continued efforts in providing and helping with the details of the ICESat data. In particular the authors wish to thank K. Barbieri, A. Brenner, J. Dimarzio and S. Bhardwaj.

## REFERENCES

[1] Zwally et. al., "ICESat's laser measurements of polar ice, atmosphere, ocean and land," *Journal of Geodynamics*, Vol. 34, No. 3-4, 2002, pp. 405-445.

[2] Luthcke, S.B., C.C. Carabajal, D.D. Rowlands, "Enhanced geolocation of spaceborne laser altimeter surface returns: parameter calibration from the simultaneous reduction of altimeter range and navigation tracking data," *Journal of Geodynamics*, Vol. 34, No. 3-4, 2002, pp. 447-475.

[3] Rowlands, D.D., D.E. Pavlis, F.G. Lemoine, G.A. Newumann, S.B. Luthcke, "The use of laser altimetry in the orbit and attitude determination of Mars Global Surveyor," *Geophysical Research Letters*, Vol. 26, No. 9, 1999, pp. 1191-1194.

[4] Luthcke, S.B., D.D. Rowlands, J.J. McCarthy, D.E. Pavlis, E. Stoneking, "Spaceborne laser-altimeter-pointing bias calibration from range residual analysis," *Journal of Spacecraft and Rockets*, Vol. 37, No. 3, 2000, pp. 374-384.

[5] Rowlands, D.D., C.C. Carabajal, S.B. Luthcke, D.J. Harding, J.M. Sauber, J.L. Bufton, "Satellite laser altimetry: on-orbit calibration techniques for precise geolocation," The Review of Laser Engineering, Vol. 28, No. 12, 2000, pp. 796-803.

[6] *GEODYN Operations Manual – 5 Volumes*, NASA/GSFC, Space Geodesy Branch, Code 926.

[7] Bae, S.and B. Schutz, "Laser pointing determination using stellar reference system in Geoscience Laser Altimeter System," American Astronautical Society (00-123), 2000.

[8] Bae, S. and B. Schutz, "GLAS Spacecraft Attitude Determination Using CCD Star Tracker and 3-axis Gyros," American Astronautical Society (99-165), 1999.

[9] Sirota, M., P. Millar, E. Ketchum, B. Schutz and S. Bae, "System to Attain Accurate Pointing Knowledge of The Geoscience Laser Altimeter," American Astronautical Society (01-003), 2001.

[10] Carabajal, C.C., D.J. Harding, J.L. Bufton, S.B. Luthcke and D.D. Rowlands, "ICESat Geolocation and Land Products Validation: Laser Altimetry Profile and Waveform Matching," International Archives of Photogrammetry and Remote Sensing, ISPRS workshop proceedings, WG I/3-WGII/2, Portland, OR, 17-19 June, 2003.